Accepted Manuscript

Identification and development of benzoxazole derivatives as novel bacterial glutamate racemase inhibitors

Prasanthi Malapati, Vagolu Siva Krishna, Radhika Nallangi, Rudraraju Reshma Srilakshmi, Dharmarajan Sriram

PII: S0223-5234(17)31119-4

DOI: 10.1016/j.ejmech.2017.12.088

Reference: EJMECH 10066

To appear in: *European Journal of Medicinal Chemistry*

Received Date: 5 October 2017

Revised Date: 27 December 2017

Accepted Date: 27 December 2017

Please cite this article as: P. Malapati, V.S. Krishna, R. Nallangi, R.R. Srilakshmi, D. Sriram, Identification and development of benzoxazole derivatives as novel bacterial glutamate racemase inhibitors, *European Journal of Medicinal Chemistry* (2018), doi: 10.1016/j.ejmech.2017.12.088.

Identification and development of benzoxazole derivatives as novel bacterial glutamate racemase inhibitors

Prasanthi Malapati, Vagolu Siva Krishna, Radhika Nallangi, Rudraraju Reshma Srilakshmi, Dharmarajan Sriram*

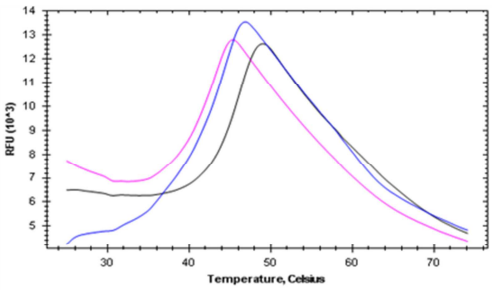

Fluorescent thermal shift assay (FTS) and enzyme screening of in house library

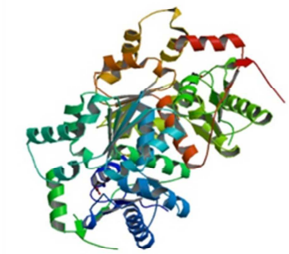

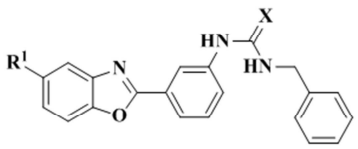

Lead 1

Δ T_m 3.2 °C , IC_{50} 20.7±0.29 µM

Lead identification

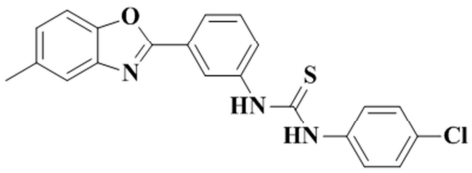

Compound 22

Synthetic chemistry approach- lead expansion

Δ T_m 6.1 °C , IC_{50} 1.1 ± 0.52 µM
MIC = 8.72 µM
Nutrient starvation = 2.5 log
Biofilm = 2.4 log
Zebra fish model = 3.4 log

We identified lead compound for M. tuberculosis glutamate racemase by thermal shift assay. We further synthesize further compounds and tested against various model of M. tuberculosis together with docking studies.

SHORT COMMUNICATIONS

Identification and development of benzoxazole derivatives as novel bacterial glutamate racemase inhibitors

Prasanthi Malapati, Vagolu Siva Krishna, Radhika Nallangi, Rudraraju Reshma Srilakshmi, Dharmarajan Sriram*

Department of Pharmacy, Birla Institute of Technology & Science-Pilani, Hyderabad Campus, Shameerpet, Jawaharnagar, RangaReddy District, Hyderabad 500 078, India

Abstract

In the present study, we attempted to develop novel class of *Mycobacterium tuberculosis* (*Mtb*) inhibitors by exploring the pharmaceutically underexploited enzyme targets which are majorly involved in cell wall biosynthesis of mycobacteria. For this purpose glutamate racemase was selected which racemizes D-glutamate from L-glutamate, a key step in peptidoglycan synthesis. Furthermore, enzyme is neither expressed nor its product, D-glutamate is produced in mammals, and hence inhibiting this enzyme will have no vulnerable effect in host organism. A library of our in-house compounds were screened against glutamate racemase using a biophysical technique; thermal shift assay and further by enzyme inhibition assay to identify **Lead 1** molecule. **Lead 1** optimization and expansion resulted in twenty four compounds. Among the synthesized compounds twelve compounds shown good enzyme inhibition than **Lead 1** (IC_{50} 20.07±0.29 µM). Among all the compounds; compound **22** (IC_{50} 1.1±0.52 µM) showed potent non-competitive mode of inhibition in enzyme assay. Further showed good susceptibility (in replicating bacteria) of MIC 8.72 µM and bactericidal time dependant kill on dormant culture. It

also exhibited significant activity in *Mtb* nutrient starvation model (2.5) and *Mtb* biofilm model (2.4) and *in vivo* M. marinum infected Zebra fish model studies (3.6) reduction at logarithmic scale.

Key words: Tuberculosis, glutamate racemase, racemization, benzoxazole, thermal shift assay screening

Contact for correspondence Tel.: +91 40663030506; fax: +91 4066303998. E-mail address: dsriram@hyderabad.bits-pilani.ac.in

Identification and development of Benzoxazole derivatives as bacterial glutamate racemase inhibitors

Prasanthi Malapati, Vagolu Siva Krishna, Radhika Nallangi, Rudraraju Reshma Srilakshmi, Dharmarajan Sriram*

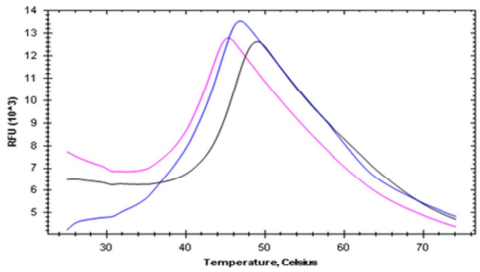

Fluorescent thermal shift assay (FTS) and enzyme screening of in house library

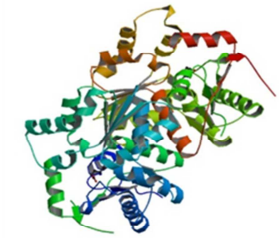

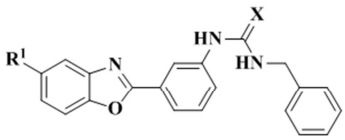

Lead 1

Δ T_m 3.2 °C , IC_{50} 20.7±0.29 µM

Lead identification

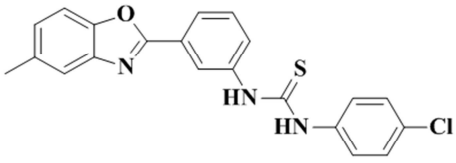

Compound 22

Synthetic chemistry approach- lead expansion

Δ T_m 6.1 °C , IC_{50} 1.1 ± 0.52 µM
MIC = 8.72 µM
Nutrient starvation = 2.5 log
Biofilm = 2.4 log
Zebra fish model = 3.4 log

1. Introduction

Tuberculosis (TB) is considered to be one of the deadly diseases in world. It's an air borne disease primarily infecting lungs caused by *Mycobacterium tuberculosis* (*Mtb*). Despite of potent drugs and treatment regimen available, emergence of drug tolerant strains led to the report of millions of deaths and new cases every year [30, 31]. As soon as the *Mtb* enters the body bacteria will be phagocytized by macrophages initiating the host immune system [1]. If the virulence of the bacteria is high Mtb can survive and replicate in host spreading to other organs through lymphatic system [2, 3]. Cellwall contributes to a major part for the virulence nature of *Mtb*. Synthetic mechanism of *Mtb* cellwall is complex and has been divided into three phases I, II, III characterized by synthesis of peptidoglycan, lipid lined intermediates and polymerization respectively. Majority of active drugs reported act on cellwall target phase III [4]. Pertaining to the development of tolerance to these drugs there is an urgency to look for alternative valid targets against *Mtb*. Phase I in cellwall formation was under exploited in drug research. Insertion of D-glutamate is very essential for the peptidoglycan formation; glutamate racemase (GR) is responsible for catalyzing racemization of L-glutamate (L-glu) to D-glutamate (D-glu). GR is an important enzyme conserved in most of the bacterial species depicting the importance of the enzyme for survivability of bacteria. There were reports for GR inhibitors against various bacteria naming few like 8-benzyl pteridine-6,7-diones, pyridodiazepine amines acting against *Staphylococcus aureus* and *Helicobacter pylori* respectively [4, 5].

In this regard this co-factor independent enzyme can be exploited as a potent target in *Mtb*. We have attempted to develop the inhibitors against GR by designing, synthesizing followed by valid screening and evaluation of compounds resulting in active drug like molecules targeting GR.

Designing of compounds started with the identification of lead compound from our in-house database using one of the biophysical technique thermal shift assay.

Results and Discussion

1.1. Lead identification by fluorescence thermal shift screening:

Ligand screening using biophysical techniques has gained popularity in current research owing to their broad range of applicability and functional relevance [6]. The fluorescence thermal shift (FTS) assay is a technique that improves the outcome of novel drug pipeline and provides a fast and reliable platform for screening and further identifying ligands in protein function or drug discovery domain[20]. In this study, we have screened our in-house ligand library of 650 molecules with structural diversity. We conducted the assay with purified *Mtb* glutamate racemase enzyme with substrate D-glu in bound and free forms against test compounds. Melt curve of protein in its free state has shown T_m at ~43.6 ^oC and in complex with D-glu at ~44.8 ^oC. Screened compounds showed a varied range ΔT_m of which **lead 1** compound has shown T_m at ~46.8 ^oC, which is showing a Δ3.2 ^oC with unbound protein and Δ2.0 ^oC with protein bound to D-glu. This result shows the competence of compound **lead 1** in stabilizing the protein from rest of the library and showing more chances for considering it as a lead compound.

Recent reports have stated that obtaining pure form of recombinant *Mtb* GR enzyme with good catalytic activity wasn't successful even by trying with different optimal purification procedures [8]. Therefore we have considered performing activity assay on same enzyme from different bacteria having more similarities with *Mtb* in terms of genetic makeup. Following the recent literature, we have considered *Bacillus subtilis* (*Bsb*) having 40% and 56% of respective sequence identity and similarity with *Mtb* and carried out the enzyme inhibitory assay for library

compounds screened by FTS method [9]. Compound **Lead 1** has shown an IC_{50} of 20.7±0.29 µM against *Bsb* glutamate racemase (**Fig.1**). In both FTS and inhibitory assay compound **Lead 1** has shown good activity, hence it was taken as a lead molecule and further optimized through structural modifications using chemical procedures.

1.2. Chemistry:

The target molecules were synthesized by two step synthetic protocol (**Scheme 1**); in first step 4-substituted-2-aminophenols (**1a-b**) were treated with 3-aminobenzoicacid (**2**) to produce corresponding substituted cyclized compounds **3a-b** (3-(benzo[d]oxazol-2-yl)aniline). In next step, the primary amine group of phenyl ring was reacted with various substituted arylisocyanates using ethanol as solvent to produce *N*, *N*-substituted urea derivatives (**4-16**); but using similar conditions for the preparation of *N*, *N*-substituted thiourea derivatives, the reactions were not successful, then we employed K_2CO_3 as base and DMF/xylene as solvents to produce *N*, *N*-substituted thiourea derivatives (**17-28**). All the analytical data (^{1}H NMR, ^{13}C NMR, and mass spectra) of synthesized compounds (both intermediates and finals) were on par with designed structures. A total twenty four compounds were synthesized as represented in (**Table 1**).

1.3. Enzyme activity assay:

Enzyme activity analysis was performed for the twenty seven compounds synthesized during hit expansion. The recombinant gene from *Bsb* was cloned, expressed and purified as described in experimental section, using pET28a+plasmid and BL21 cells as expression vector followed by purification and confirmation through SDS-PAGE. A reaction mixture containing glutamate racemase, D-glu and test compounds was incubated and the product resulted (L-glu) was reacted

with L-Glutamate dehydrogenase (GDH) and NAD^+ where the inhibitory activity was determined by employing an coupled assay by measuring the absorption readings of NADH formed after GDH mediated conversion from NAD^+ at λ_{340}. The IC_{50} values of compounds were shown in **Table 1**. A total of thirteen compounds have shown activity less than 25 µM, of which except two compounds rest were active below 10 µM concentration. Compounds **16, 19, 21** and **22** have shown activity <5 µM. Most of the compounds showing good activity have thiourea substitution, out of twelve compounds belonging to thiourea group, eight compounds have shown less than 10 µM activity and one has shown activity of 22.8±0.42 µM. Most potent of the series, compound **22** showed an IC_{50} of 1.1±0.52 µM which is less inhibitory concentration than lead compound (IC_{50} of 20.7±0.29 µM) by twenty times. The log dose response curve of most potent compound **22** of series was shown in (**Fig. 2**).

1.4. Molecular docking and dynamic studies:

Molecular docking is one technique which gives the all the possible interactions of ligand with the protein and suggests the possibility of a compound to accept as an inhibitor. In this study we have performed the inhibitory activity on glutamate racemase of *Bsb*, stillthere is requirement for further validation of results. We performed all the docking analysis using Schrodinger software. We have selected substrate (D-glu) bound glutamate racemase crystal structures of both organisms from protein data bank namely PDB ID: 5HJ7 (*Mtb*) and 1ZUW (*Bsb*), the protein alignment of both proteins has an root mean square deviation (rmsd) 1.33 Å. We tried docking of energy minimized ligands into substrate binding site but was unsuccessful, hence we have tried docking in allosteric sites (assuming the inhibitors act through allosteric site) generated using an in-built program called SiteMap. SiteMap is considered to be a tool that helps in interpreting the additional important sites of the protein which help in increasing the

probability of finding the drugs in drug research areas. In the present study, five sites were identified in the each crystal structures of proteins. Among all generated sites considering the site-scores, **site 1** in both the proteins was selected for further docking studies. **Site 1** of *Mtb* has the site-score 0.8203 and was surrounded by hydrophobic residues namely Pro43, Pro46, Pro146, Val149 and Leu250 and few polar amino acid residues Glu 153, Ser13, Thr39, Thr119 and His187. In *Bsb* **site 1** having site-score 0.6982 was boarded by hydrophobic residues Pro41, Pro44, Pro146, Val149 and Cys40 and also by polar residues like Thr37, Thr118 and Gln245 respectively. The allosteric sites considered in both the bacteria are lined by the identical residues (**Supplementary Fig. 1**). Therefore the compounds show similar kind of action in both the bacteria binding in these sites.

Compounds were docked into allosteric sites of both the crystal structures. We have superimposed both the proteins bound with ligand **22** using superimposition module in Schrodinger shown in **Fig. 3**. In this study, we have studied the docking orientation of most active compound **22** in both the crystal structures. The binding orientation showed a two H-bond interactions with allosteric residue Glu153 in both the crystal structures with NH moiety of compound (**Fig. 4).** Along with previous interactions, the orientation was stabilized by hydrophobic and polar interactions. The compound was very well fit into the cavity of both proteins retaining similar kind of interaction with docking scores of -5.075 kcal/mol and -3.457 kcal/mol respectively in *Bsb* and *Mtb*. Hence we infer that there established a correlation of inhibitory activity of compound **22** in both the organisms.

Molecular dynamics simulations help in understanding the structure and function of macromolecules at basic level. Simulations provide every minute detail about every particle/atom movement with respect to time. This will help in answering the questions arising

on deviation and fluctuation pattern of protein. [We have subjected the Compound **22** bound in 5HJ7 and 1ZUW protein complexes to a 10 ns simulation using Desmond. The deviation and fluctuation patterns were measured in terms of rmsd and rmsf (root mean square fluctuation). Rmsd of protein (C_α) and ligand obtained during 10 ns simulation for the 1ZUW crystal structure were within average of ~1.21 Å and ~0.9 Å and for 5HJ7 both C_α and ligand were within an average of ~1.35 Å and ~0.82 Å respectively (**Supplementary Fig. 2)**. Rmsf analysis inferred that proteins and ligand at their binding site have shown negligible fluctuations with ~1.36 Å and 1.41 Å respectively for 5HJ7 and 1ZUW (**Supplementary Fig. 3**).

1.5. Thermal shift assay:

FTS is known majorly for establishing the stability data of a protein. Based on the principle involved, this tool can also be used to characterize the compound or ligand and its effects on protein by studying the shift in melt temperature (ΔT_m) in the presence of different ligands. A positive shift in (T_m) in comparison with protein in its free state (unbound) indicates the stability enhancement of protein and a negative shift indicates the destabilization of protein. Based on this principle, mode of inhibition can be categorized into three [22]. First is competitive mode of inhibition, where the inhibitor induces a negative shift in T_m. Second, uncompetitive inhibition showing a positive ΔT_m only in the presence of substrate-bound state and in the absence of substrate no change is recorded. Third is the non-competitive way of inhibition, here a positive shift in melt temperature will be seen irrespective of substrate existence in protein [22].

We have analysed inhibitor characterization in *Mtb* glutamate racemase. The thermal shift analysis of active compound **22** shows a clear non-competitive mode of inhibition. The protein unbound form showed T_m ~43.7 ^oC and bound form at ~45.1 ^oC respectively. The compound **22** showed T_m ~49.8 ^oC with unbound protein and T_m ~51.9 ^oC with protein bound with substrate

(**Fig. 5**). These melt temperature shifts (ΔT_m) were higher compared to that of **lead 1** (reported above). This infers that the protein and protein-substrate complex were more stabilized in the presence of compound **22** when compared to **lead 1**.

1.6. Mtb susceptibility testing:

Determining whole cell activity against *Mtb* is an important factor in drug development research against tuberculosis. Microplate Alamar Blue Assay (MABA) is an economic and expeditious assay determining the drug susceptibility against replicating *Mtb* in quantitative terms [23]. MABA assay was performed for all the synthesized compounds to determine the minimum inhibitory concentration (MIC) of each compound when tested at concentrations varying from 50 μg/mL to 0.78 μg/mL. MIC values of the test compounds and the standard drugs (Isoniazid, Ethambutol and Rifampicin) were represented in **Table 1**. Compounds **17, 18, 19, 22** and **23** having thiourea substitution, have shown inhibition below 10 μM. Of which four compounds (**17, 18, 19** and **23**) were more active than standard drug Ethambutol (MIC 7.89 μM). Compounds **17, 18, 23** have shown more whole cell inhibition compared to that of enzyme inhibition. To our assumption, this conjugate effect might be due to an additional pathway inhibition. Few compounds in spite of having good activity profile in enzyme assay failed to inhibit the whole organism, where the reason could be the efflux of compound by the complex cellwall of bacteria. Efflux mechanism of bacteria is the major hurdle for drug susceptibility mediated by major facilitator superfamily (MFS) proteins or antibiotic-modifying, degrading enzymes and transporters [26]. Reports were available stating that combining efflux pump inhibitors verapamil and piperine has increased the intake of drug by the bacteria than in their absence [28, 29]. Assuming that the failure of compounds in replicating bacteria might be due to efflux of drug, the compounds **4, 6**, **13**, **14**, **16**, **20**, **21**, **22** and **24** active in enzyme assay were

tested for their susceptibility in the presence of verapamil and piperine. Compounds **16**, **20**, **21** and **22** have shown drastic increase in activity against *Mtb* than as individual drugs (**Table 1**). The remaining compounds haven't showed any difference in their activities and the reason might be the lack of permeability of compounds across the complex lipid bacterial cellwall. The most active molecule in enzyme assay, compound **22** (IC_{50} of 1.1±0.52 μM) has shown an MIC of 8.72 μM in the absence of efflux pump inhibitors and 2.01 μM with a difference of four times in the presence of efflux pump inhibitors.

1.7. Mycobacterium tuberculosis nutrient starved dormancy model:

Mtb attains dormancy and phenotypically develop drug resistance when it undergoes stress within the host. Inability of currently available and developing drugs to kill persistent *Mtb* is a major hindrance to find therapeutic possibility to diminish tuberculosis (TB). An *in vitro* stress model that generates dormancy in *Mtb* cells is required to reveal the essential metabolics that allow bacteria to undergo into latent phase in turn help in identification and screening of novel drugs to kill persistent bacteria. Nutrient starvation is one such model which creates the dormancy in bacteria by starving culture in phosphate buffer saline (PBS) for 6 weeks. The dormant culture was tested with selected compounds at concentration of 10 μg/mL [14]. Based on enzyme and MABA assay activities, compounds **17, 18, 19** and **22** were selected to test against dormant assays. Rifampicin (RIF), Isoniazid (INH) and Moxifloxacin (MOXI) were used as reference compounds. The comparative inhibitory activity plots in nutrient starvation model were shown in **Fig. 6**. Compounds **17, 18** and **22** have shown a similar inhibition with a log reduction of 2.5 (with control), 1.4 (with INH), 0.8 (with RIF) and 0.3 with (MOXI). Compound **19** has shown a difference of 0.2 log reduction when compared to other test compounds. Test

229 compounds have shown similar inhibition with less variation with good activities in active and
230 dormant model.

231 ***1.8. Mtb time-Kill Kinetics determination:***

232 It's essential to study the pharmacodynamics of novel drug molecules by analyzing the kill of
233 drug molecule at different concentrations against time. This aids in determining the
234 concentration-dependent and time-dependent bactericidal activities of drug molecules. Minimum
235 bactericidal concentration (MBC) is defined as the concentration at which inhibitor shows three
236 fold inhibition of bacteria, incubated for 21 days. To determine MBC, the compound at different
237 concentrations (decided according to MIC value) was incubated for 21 days and recorded the
238 readings at different time points (0, 7, 15 and 21 days). A compound is said to be bactericidal if
239 MBC is within 4 folds of its MIC and bacteriostatic if it's more than four folds [15]. Bactericidal
240 compounds exhibit two types of kill namely time dependant and concentration dependant. We
241 have used starved culture (depleted of nutrients for 2 weeks) for assay. Compounds **17, 18, 19**
242 and **22** were tested for determining their kill kinetics. Compounds **19** and **22** have shown
243 bactericidal mode of inhibition with their MBC values 27.47 µM and 25.38 µM respectively. We
244 have represented the kinetics study of compound **22** in **Fig. 7.** It shows a time dependant kill,
245 where one can observe the kill increased with time irrespective of concentration.

246 ***1.9. Mtb biofilm assay:***

247 *Mtb* forms organized biofilm containing mycolic-acid-rich extracellular matrix. Assessment of
248 *Mtb* biofilm cultures to available potent antibiotics (INH and RIF) resulted in the survival of
249 cells confirming that these biofilms harbor the drug-tolerant cells [24]. Compounds **17, 18, 19**
250 and **22** were tested for their activity on biofilm at concentration of10 µg/mL. Reference drugs

INH, RIF and MOXI have shown a log reduction of 1.2, 1.5 and 2.0 respectively compared to control. Test compounds **17, 18** have shown 0.8 and compounds **19** and **22** have shown log reduction of 0.4 and 2.4 respectively (**Fig. 8**). These values infer that compound **22** is active in both active and dormant forms of bacteria.

1.10. In-vivo activity testing assay by Mycobacterium marinum infected adult zebrafish:

Identification of novel antimicrobial compounds can be accelerated using the zebrafish model, especially in tuberculosis. Activity and dosage of antibiotics in zebrafish closely be like characteristics in humans. This model has emerged to be the most economic and reliable model for researches to study the *in vivo* activity of new drug compounds [25]. In this study, zebrafish is infected with *Mycobacterium marinum* (belongs to same family genetically). Active molecule **22** at *in vitro* level was tested for *in vivo* inhibitory activity using adult zebra fish model. Standard compounds INH and MOXI have shown reductions of 2.5 and 2.4 in log scale and test compound **22** has shown 3.4 log reduction with control, which is more than standards (**Fig. 9**).

1.11. Cytotoxicity determination:

Toxicity testing of new compounds is very much essential for drug development process, can be observed by *in vivo* and *in vitro* models. In this study, we have tested toxicity using *in vitro* technique employing cell lines by MTT (3-(4,5-Dimethylthiazol-2-yl)-2,5-Diphenyltetrazolium Bromide) assay. RAW 246.7 cell lines were used for experimental studies [18]. All the compounds were tested at a concentration of 25 µM and the percentage inhibition were found to be in different ranges as shown in **table 1**. Hence most of the compounds are devoid of effects on metabolism.

2. Conclusion

In the current scenario persistence, resistance and co-infection are the foremost drawbacks that hinder the tuberculosis treatment regimen. In present work, we have focused on combating persistence and resistance by targeting a novel enzyme vital for the bacterial survival. We have we have identified and optimized through hit expansion. Compounds which showed good *in vitro* and *in vivo* activities belong to thiourea family. Compound **22** (1-(4-chlorophenyl)-3-(3-(5-methylbenzo[d]oxazol-2-yl)phenyl)thiourea) was proven to be the most potent molecule of series in both *in vitro* and *in vivo* evaluation studies. This data was supported by molecular docking and simulation studies, both the compounds retained similar kind of interactions with amino acid residues. There were some compounds which are active in vitro but were unsuccessful on whole cell organism, one of the drawback can be the strong efflux nature of cell wall. Further, there were few compounds showing very food whole organism inhibition than enzyme inhibition, these might be targeting an additional pathway for inhibition. These compounds need further studies to answer all questions in drug discovery. Further optimization of compounds can results in still better compounds for treating tuberculosis.

3. Experimental Section

3.1. Thermal shift assay:

Thermal stability assays were performed as reported in literature [7]. The reaction was carried out in 0.2 mL PCR tubes (Bio-Rad) containing a 25 µL mixture of *Mtb* glutamate racemase (0.2 mg/mL concentration), test compounds (diluted in DMSO < 2 %v/v), 2 mM D-glutamate and buffer (100 mM Tris HCl, 100 mM NaCl, pH 8.0) and 6.25x SYPRO orange dye (Sigma). The reaction was using real-time PCR thermal cycler (Bio-Rad). The protocol was set with heating from 20 to 80 ^{o}C with a gradient of 0.02 ^{o}C/s. All the reactions were carried in duplicates. Changes in fluorescence of SYPRO orange dye were monitored, to determine the

unfolding pattern of protein. T_m values were obtained from the minima of the first derivative (−dF/dt) plots of unfolding protein curves using an in-built function in Bio-Rad prime PCR software.

3.2. Chemistry :

Reagents obtained from commercial sources were used directly without further purification. Reactions were carried out under inert atmosphere of nitrogen or argon. All the reactions were monitored by thin layer chromatography (TLC) on silica gel 40 F254 (Merck, Darmstadt, Germany) coated on aluminium plates. ^{1}H and ^{13}C NMR spectra were recorded on a Bruker AM-400 NMR spectrometer, Bruker BioSpin Corp., Germany. Chemical shifts are in parts per million (ppm) using tetramethylsilane as internal standard. Temperatures are reported in degrees Celsius and are uncorrected. Compounds were analysed for C, H, N and analytical results obtained were within ±0.4% of the calculated values for the formula shown. Molecular weights of the synthesised compounds were checked by (Shimadzu, LCMS-2020) ESI-MS method.

3.2.1. General procedure for the preparation of 3a-b: 3-amiobenzoicacid (**2**) (1.0 equiv), compound **1a-b** (1.1 equiv) and PPA (10 volumes) mixture was allowed to reflux at 185 °C for 6 hours. After the completion of reaction, the contents were cooled and neutralized with cold 6N NaOH solution. The precipitate formed was filtered and further continued for heating in DMF at 60 °C for 15 minutes, and contents were transferred into crushed ice. The solid was filtered and washed with cold ethanol and diethyl ether to get the corresponding recrystallized compound **3a-b** respectively.

3.2.2. Synthesis of 3-(benzo[d]oxazol-2-yl)aniline (3a): The compound was synthesized according to above general procedure using 2-aminophenol (1 g**,** 9.17 mmol), 3-

amiobenzoicacid (0.9 g, 6.84 mmol) and PPA (10 mL) to obtain 3-(benzo[d]oxazol-2-yl)aniline (1.6 g,73%) as pale yellow solid. ^{1}H NMR (400 MHz, $CDCl_3$): δ 8.29 (s, 1H), 8.11-7.89 (m, 3H), 7.58-7.39 (m, 4H), 6.87 (s, 2H). ^{13}C NMR (100 MHz, $CDCl_3$): δ 163.3, 151.3 (2C), 143.6, 132.7, 128.6, 124.9 (2C), 119.5 (3C), 116.3, 109.9. MS(ESI) *m/z* 211 $[M+H]^+$. Anal calcd for $C_{13}H_{10}N_2O$: C, 74.27; H, 4.79; N, 13.33; Found: C, 74.34; H, 4.78; N, 13.35.

3.2.3. Synthesis of 3-(5-methylbenzo[d]oxazol-2-yl)aniline (3b): The compound was synthesized according to above general procedure using 2-amino-4-methylphenol (1g**,** 8.13mmol), 3-amiobenzoicacid (0.9 g, 6.84 mmol) and PPA (10 mL) to obtain 3-(5-methylbenzo[d]oxazol-2-yl)aniline (1.8 g,71%) as white solid. ^{1}H NMR (400 MHz, $CDCl_3$): δ 8.42 (s, 1H), 8.22 (s, 1H), 7.92-7.52 (m, 5H), 6.94 (s, 2H), 2.45 (s, 3H). ^{13}C NMR (100 MHz, $CDCl_3$): δ 162.9, 149.2, 145.6, 140.8, 135.2, 132.7, 127.6 (2C), 118.5 (3C), 113.8, 108.7, 22.3. MS(ESI) *m/z* 225 $[M+H]^+$. Anal calcd for $C_{14}H_{12}N_2O$: C, 74.98; H, 5.39; N, 12.49; Found: C, 74.82; H, 5.38; N, 12.47.

3.2.4. General procedure for the preparation of compounds 4-15: To the mixture of compounds **3a-b** (1.0 equiv), DIPEA (2.0 equiv) was added with the corresponding arylisocyanate (1.25 equiv) in DMF. After the reaction has completed, mixture was added to EtOAc followed by washing with water, Brine solution and distilled under reduced pressure to obtain product. The crude product was purified by column chromatography using EtOAc/hexane as eluent to obtain pure compounds **4-15**.

3.2.5. Synthesis of 1-(3-(5-methylbenzo[d]oxazol-2-yl)phenyl)-3-phenylurea (4): The compound was synthesized according to above general procedure using 3-(5-methylbenzo[d]oxazol-2-yl)aniline (1.5 g, 6.69 mmol), DIPEA (1. 8 g, 12.62 mmol) and isocyanatobenzene (1.2 g, 10.05 mmol) to yield 1-(3-(5-methylbenzo[d]xazol-2-yl)phenyl)-3-

phenylurea (1.8 g, 77%) as grey solid. Mp: 240-243 ^{o}C. ^{1}H NMR (400 MHz, $CDCl_3$): δ 10.87 (s, 2H), 8.31 (s, 1H), 7.92 (d, J = 7.6 Hz, 1H), 7.84–7.72 (m, 4H), 7.63 (d, J = 7.2 Hz, 2H), 7.58–7.49 (m, 4H), 2.39 (s, 3H); ^{13}C NMR (100 MHz, $CDCl_3$): δ 174.6, 160.2, 144.9, 141.4, 140.6, 135.2, 135.0, 133.3, 132.4(2C), 130.8, 129.4, 127.8(2C), 125.9, 125.6, 125.2, 124.6, 120.3, 116.3, 22.9. MS(ESI) *m/z* 344 $[M+H]^+$. Anal calcd for $C_{21}H_{17}N_3O_2$: C, 73.45; H, 4.99; N, 12.24% Found C, 73.58; H, 4.98; N, 12.26%.

3.2.6. Synthesis of 1-(4-chlorophenyl)-3-(3-(5-methylbenzo[d]oxazol-2-yl)phenyl)urea (5): The compound was synthesized according to above general procedure using 3-(5-methylbenzo[d]oxazol-2-yl)aniline (1.5 g, 6.69 mmol), DIPEA (1.8 g, 12.62 mmol) and 1-chloro-4-isocyanatobenzene (1.3 g, 8.51 mmol) to yield 1-(4-chlorophenyl)-3-(3-(5-methylbenzo[d]oxazol-2-yl)phenyl)urea (1.9 g, 73%) as white solid. M.p:181-183 ^{o}C. ^{1}H NMR (400 MHz, DMSO-d_6): δ 9.34 (s, 2H), 8.52 (s, 1H), 7.85 (d, J = 8.0 Hz, 1H), 7.8 (d, J = 8.4 Hz, 1H), 7.75 (t, J = 8.0 Hz, 1H), 7.71–7.62 (m, 5H), 7.43 (d, J = 8.0 Hz, 2H), 3.82 (s, 3H); ^{13}C NMR (100 MHz, DMSO-d_6): δ 176.3, 163.3, 154.3, 146.4, 139.6, 137.5, 135.6, 134.8, 133.2, 132.0(2C), 131.8, 131.3, 129.9(2C), 128.6, 127.4, 126.0, 120.4, 113.8, 60.4, 23.2. MS(ESI) *m/z* 379 $[M+H]^+$. Anal calcd for $C_{21}H_{16}ClN_3O_2$: C, 70.76; H, 5.13; N, 11.25 Found C, 70.88; H, 5.14; N, 11.23.

3.2.7. Synthesis of 1-(3-(benzo[d]oxazol-2-yl)phenyl)-3-(4-methoxyphenyl)urea (6): The compound was synthesized according to above general procedure using 3-(benzo[d]oxazol-2-yl)aniline (1.3 g, 6.19 mmol), DIPEA (1.8 g, 12.62 mmol) and 1-isocyanato-4-methoxybenzene (1.2 g, 8.02 mmol) to yield 1-(3-(benzo[d]oxazol-2-yl)phenyl)-3-(4-methoxyphenyl)urea (1.9 g, 86%) as grey solid. M.p:228-230 ^{o}C. ^{1}H NMR (400 MHz, DMSO-d_6): δ 10.25 (s, 2H), 8.40 (s, 1H), 7.89 (d, J = 8.0 Hz, 2H), 7.76–7.63 (m, 3H), 7.56–7.48 (m, 4H), 7.18 (t, J = 7.6 Hz, 2H),

3.96 (s, 3H); ^{13}C NMR (100 MHz, DMSO-d_6): δ 172.4, 162.4, 150.2, 145.8, 141.3, 138.2, 136.4, 135.1, 134.6, 134.1(2C), 133.2, 131.4, 128.2(2C), 126.4(2C), 125.3, 124.2, 119.4, 114.6. MS(ESI) *m/z* 360 $[M+H]^+$. Anal calcd for $C_{21}H_{17}N_3O_3$: C, 70.18; H, 4.77; N, 11.69 Found C, 70.28; H, 4.76; N, 11.66.

3.2.8. Synthesis of 1-(3-(benzo[d]oxazol-2-yl)phenyl)-3-(4-nitrophenyl)urea (7): The compound was synthesized according to above general procedure using 3-(benzo[d]oxazol-2-yl)aniline (1.3 g, 6.19 mmol), DIPEA (1.8 g, 12.62 mmol) and 1-isocyanato-4-nitrobenzene (1.3 g, 7.98 mmol) to yield 1-(3-(benzo[d]oxazol-2-yl)phenyl)-3-(4-nitrophenyl)urea (1.9 g, 84%) as yellow solid. M.p:250-252 ^{o}C. ^{1}H NMR (400 MHz, DMSO-d_6): δ 10.08 (s, 2H), 8.45 (s, 1H), 8.19 (d, J = 8.4 Hz, 2H), 7.94 (d, J = 8.0 Hz, 2H), 7.88 (d, J = 7.6 Hz, 1H), 7.82 (d, J = 8.0 Hz, 2H), 7.78–7.71 (m, 3H), 7.69 (t, J = 7.6 Hz, 1H); ^{13}C NMR (100 MHz, DMSO-d_6): δ 167.4, 156.3, 152.3, 146.6, 143.5, 139.3, 136.4, 134.8(2C), 133.2, 132.8(2C), 131.2, 130.5, 130.0, 128.4, 126.2, 125.9, 120.9, 116.7. MS(ESI) *m/z* 375 $[M+H]^+$. Anal calcd for $C_{20}H_{14}N_4O_4$: C, 64.17; H, 3.77; N, 14.97 Found C, 64.28; H, 3.78; N, 14.95.

3.2.9. Synthesis of 1-(3-(benzo[d]oxazol-2-yl)phenyl)-3-benzylurea (8): The compound was synthesized according to above general procedure using 3-(benzo[d]oxazol-2-yl)aniline (1.3 g, 6.19 mmol), DIPEA (1.8 g, 12.62 mmol) and (isocyanatomethyl)benzene (1.1 g, 9.6 mmol) to yield 1-(3-(benzo[d]oxazol-2-yl)phenyl)-3-benzylurea (2.0 g, 88%) as brown solid. M.p:243-245 ^{o}C. ^{1}H NMR (400 MHz, $CDCl_3$): δ 10.27 (s, 2H), 8.48 (s, 1H), 7.94 (d, J = 8.0 Hz, 1H), 7.88 (t, J = 7.6 Hz, 2H), 7.72 (d, J = 7.6 Hz, 1H), 7.68–7.56 (m, 3H), 7.42–7.26 (m, 5H), 5.08 (s, 2H); ^{13}C NMR (100 MHz, $CDCl_3$): δ 183.9, 163.4, 154.3, 144.3, 142.4, 137.9, 135.6, 135.1, 134.3(2C), 129.4, 128.7(2C), 127.1, 126.2, 125.4, 125.0, 124.3, 120.4, 113.8, 62.6. MS(ESI)

m/z 360 $[M+H]^+$. Anal calcd for $C_{21}H_{17}N_3O_2$: C, 73.45; H, 4.99; N, 12.24 Found C, 73.52; H, 4.98; N, 12.21.

3.2.10. Synthesis of 1-(4-methoxyphenyl)-3-(3-(5-methylbenzo[d]oxazol-2-yl)phenyl)urea (9)*:* The compound was synthesized according to above general procedure using 3-(5-methylbenzo[d]oxazol-2-yl)aniline (1.5 g, 6.69 mmol), DIPEA (1.8 g, 12.62 mmol) and 1-isocyanato-4-methoxybenzene (1.5 g, 9.1 mmol) to yield 1-(4-methoxyphenyl)-3-(3-(5-methylbenzo[d]oxazol-2-yl)phenyl)urea (2.1 g, 87%) as grey solid. M.p:228-230 ^oC. ^1H NMR (400 MHz, DMSO-d_6): δ 9.25 (s, 2H), 8.44 (s, 1H), 7.81 (d, J = 8.0 Hz, 1H), 7.77 (d, J = 8.4 Hz, 1H), 7.72 (t, J = 8.0 Hz, 1H), 7.67–7.60 (m, 5H), 7.21 (d, J = 7.6 Hz, 2H), 3.94 (s, 3H), 2.46 (s, 3H); ^{13}C NMR (100 MHz, DMSO-d_6): δ 176.3, 163.3, 154.3, 146.4, 139.6, 137.5, 135.6, 134.8, 133.2, 132.0(2C), 131.8, 131.3, 129.9(2C), 128.6, 127.4, 126.0, 120.4, 113.8, 60.4, 23.2. MS(ESI) *m/z* 374 $[M+H]^+$. Anal calcd for $C_{22}H_{19}N_3O_3$: C, 70.76; H, 5.13; N, 11.25 Found C, 70.88; H, 5.14; N, 11.28.

3.2.11. Synthesis of 1-(3-(benzo[d]oxazol-2-yl)phenyl)-3-(4-chlorophenyl)urea (10): The compound was synthesized according to above general procedure using 3-(benzo[d]oxazol-2-yl)aniline (1.3 g, 6.19 mmol), DIPEA (1.8 g, 12.62 mmol) and 1-chloro-4-isocyanatobenzene (1.3 g, 8.51 mmol) to yield 1-(3-(benzo[d]oxazol-2-yl)phenyl)-3-(4-chlorophenyl)urea (1,9 g, 85%) as white solid. M.p:175-177 ^oC. ^1H NMR (400 MHz, $CDCl_3$): δ 10.29 (s, 2H), 8.46 (s, 1H), 7.94 (t, J = 8.0 Hz, 2H), 7.82 (d, J = 7.6 Hz, 1H), 7.76 (t, J = 8.0 Hz, 1H), 7.69–7.60 (m, 3H), 7.56 (d, J = 7.6 Hz, 2H), 7.44 (d, J = 8.0 Hz, 2H); ^{13}C NMR (100 MHz, $CDCl_3$): δ 174.4, 160.5, 148.7, 144.9, 137.5, 136.4, 135.3, 134.9, 134.3, 133.2(2C), 132.7, 131.6, 130.2(2C), 127.3, 125.2(2C), 120.6, 117.0. MS(ESI) *m/z* 364 $[M+H]^+$. Anal calcd for $C_{20}H_{14}ClN_3O_2$: C, 66.03; H, 3.88; N, 11.55 Found C, 66.18; H, 3.89; N, 11.53.

3.2.12. Synthesis of 1-(4-fluorophenyl)-3-(3-(5-methylbenzo[d]oxazol-2-yl)phenyl)urea (11): The compound was synthesized according to above general procedure using 3-(5-methylbenzo[d]oxazol-2-yl)aniline (1.5 g, 6.69 mmol), DIPEA (1.8 g, 12.62 mmol) and 1-fluoro-4-isocyanatobenzene (1.2g, 9.2 mmol) to yield 1-(4-fluorophenyl)-3-(3-(5-methylbenzo[d]oxazol-2-yl)phenyl)urea (2.0 g, 88%) as pale brown solid. M.p:169-171 ^{o}C. ^{1}H NMR (400 MHz, DMSO-d_6): δ 10.71 (s, 2H), 8.46 (s, 1H), 7.87 (d, J = 8.0 Hz, 1H), 7.74–7.62 (m, 3H), 7.56 (d, J = 7.6 Hz, 1H), 7.54–7.46 (m, 3H), 7.36 (d, J = 8.0 Hz, 2H), 2.43 (s, 3H); ^{13}C NMR (100 MHz, DMSO-d_6): δ 174.3, 160.4, 144.7, 143.4, 139.6, 137.3, 136.2, 134.6, 133.0, 132.6(2C), 131.8, 128.5, 127.4(2C), 126.8, 125.2, 123.9, 120.8, 116.9, 22.4. MS(ESI) *m/z* 362 $[M+H]^+$. Anal calcd for $C_{21}H_{16}FN_3O_2$: C, 69.80; H, 4.46; N, 11.63 Found C, 69.88; H, 4.45; N, 11.65.

3.2.13. Synthesis of 1-(3-(benzo[d]oxazol-2-yl)phenyl)-3-phenylurea (12): The compound was synthesized according to above general procedure using 3-(benzo[d]oxazol-2-yl)aniline (1.3 g, 6.19 mmol), DIPEA (1.8 g, 12.62 mmol) and isocyanatobenzene (1.2 g, 10.05 mmol) to yield 1-(3-(benzo[d]oxazol-2-yl)phenyl)-3-phenylurea (1.7 g, 83%) as grey solid. M.p:210-212 ^{o}C. ^{1}H NMR (400 MHz, DMSO-d_6): δ 10.26 (s, 2H), 8.46 (s, 1H), 7.96 (d, J = 8.0 Hz, 1H), 7.84 (t, J = 8.0 Hz, 2H), 7.72 (d, J = 7.6 Hz, 1H), 7.63–7.56 (m, 3H), 7.48–7.36 (m, 4H), 7.22 (t, J = 8.0 Hz, 1H); ^{13}C NMR (100 MHz, DMSO-d_6): δ 176.4, 162.9, 154.2, 144.7, 142.6, 142.4, 138.5, 137.6, 136.0, 133.9(2C), 133.0, 130.6, 128.3, 127.8(2C), 126.3, 120.3, 119.3, 115.9. MS(ESI) *m/z* 330 $[M+H]^+$. Anal calcd for $C_{20}H_{15}N_3O_2$: C, 72.94; H, 4.59; N, 12.76 Found C, 72.81; H, 4.58; N, 12.78.

3.2.14. Synthesis of 1-(3-(benzo[d]oxazol-2-yl)phenyl)-3-(4-fluorophenyl)urea (13): The compound was synthesized according to above general procedure using 3-(benzo[d]oxazol-

2-yl)aniline (1.3 g, 6.19 mmol), DIPEA (1.8 g, 12.62 mmol) and fluoro-4-isocyanatobenzene (1.0g, 8.7 mmol) to yield 1-(3-(benzo[d]oxazol-2-yl)phenyl)-3-(4-fluorophenyl)urea (1.8 g, 81%) as grey solid. M.p:180-182 ^{o}C. ^{1}H NMR (400 MHz, DMSO-d_6): δ 9.00 (s, 1H), 8.73 (s, 1H), 8.12 (s, 1H), 8.84–8.73 (m, 3H), 7.54–7.36 (m, 6H), 7.12 (t, J = 8.0 Hz, 2H); ^{13}C NMR (100 MHz, DMSO-d_6): δ 178.6,156.8, 152.1, 144.2, 143.1, 136.5, 131.2, 127.9, 127.4, 126.1, 123.1, 122.7, 122.4 (3C), 120.5, 115.4, 113.2 (3C), 111.2 . MS(ESI) *m/z* 348 $[M+H]^+$. Anal calcd for $C_{20}H_{14}FN_3O_2$: C, 69.16; H, 4.06; N, 12.10 Found C, 69.24; H, 4.07; N, 12.08.

3.2.15. Synthesis of 1-(3-(benzo[d]oxazol-2-yl)phenyl)-3-(p-tolyl)urea (14): The compound was synthesized according to above general procedure using 3-(benzo[d]oxazol-2-yl)aniline (1.3 g, 6.19 mmol), DIPEA (1.8 g, 12.62 mmol) and 1-isocyanato-4-methylbenzene (1.2 g, 9.0 mmol) to yield 1-(3-(benzo[d]oxazol-2-yl)phenyl)-3-(p-tolyl)urea (1.9 g, 88%) as white solid. M.p:164-166 ^{o}C. ^{1}H NMR (400 MHz, DMSO-d_6): δ 9.21 (s, 2H), 8.41 (s, 1H), 7.89 (d, J = 8.0 Hz, 1H), 7.81–7.72 (m, 2H), 7.67–7.56 (m, 3H), 7.54–7.45 (m, 3H), 7.33 (t, J = 8.0 Hz, 2H), 2.46 (s, 3H); ^{13}C NMR (100 MHz, DMSO-d_6): δ 174.6, 162.6, 154.0, 146.5, 136.4, 135.3, 134.8, 134.0, 133.4, 132.3(2C), 130.5, 129.4, 128.2(2C), 126.8, 126.4, 124.5, 121.3, 117.4, 22.6. MS(ESI) *m/z* 344 $[M+H]^+$. Anal calcd for $C_{21}H_{17}N_3O_2$: C, 73.45; H, 4.99; N, 12.24 Found C, 73.56; H, 4.98; N, 12.26.

3.2.16. Synthesis of 1-(3-(benzo[d]oxazol-2-yl)phenyl)-3-isopropylurea (***15***): The compound was synthesized according to above general procedure using 3-(benzo[d]oxazol-2-yl)aniline (1.3 g, 6.19 mmol), DIPEA (1.8 g, 12.62 mmol) and 2-isocyanatopropane (0.7 g, 8.2 mmol) to yield 1-(3-(benzo[d]oxazol-2-yl)phenyl)-3-isopropylurea (1.5 g, 78%) as pale red solid. M.p:174-176 ^{o}C. ^{1}H NMR (400 MHz, DMSO-d_6): δ 10.17 (s, 1H), 9.43 (s, 1H), 8.36 (s, 1H), 7.84 (d, J = 8.0 Hz, 1H), 7.74 (d, J = 8.4 Hz, 2H), 7.67–7.56 (m, 3H), 7.36 (t, J = 8.0 Hz,

458 1H), 3.85–3.81 (m, 1H), 1.33 (d, J = 8.8 Hz, 6H); ^{13}C NMR (100 MHz, DMSO-d_6): δ 171.9,
459 160.2, 154.4, 143.4, 136.4, 135.3, 135.0, 133.3, 129.3, 127.6, 126.1, 125.4, 118.6, 115.3, 54.6,
460 24.6(2C). MS(ESI) *m/z* 296 $[M+H]^+$. Anal calcd for $C_{17}H_{17}N_3O_2$: C, 69.14; H, 5.80; N, 14.23
461 Found C, 69.26; H, 5.81; N, 14.25.

462 ***3.2.17. General procedure for the preparation of compounds 16-27:*** To a solution of
463 compounds **3a-b** (1.0 equiv) and the corresponding arylisothiocyanate (1.3 equiv) in
464 DMF:xylene (4:1), potassium carbonate (2.0 equiv) was added with stirring. The whole reaction
465 was carried out under microwave irradiation conditions (temperature 110 °C) for about 30
466 minutes. The contents of flask were poured into the crushed ice for cooling and the resulted
467 precipitate was filtered and washed twice with ethanol. The crude residue was further purified
468 by column chromatography using ethylacetate/hexane as eluent to get the corresponding pure
469 compounds **16-27**.

470 ***3.2.18. Synthesis of 1-(3-(Benzo[d]oxazol-2-yl)phenyl)-3-benzylthiourea (16):*** The
471 compound was synthesized according to above general procedure using 3-(benzo[d]oxazol-2-
472 yl)aniline (1.3 g, 6.19 mmol), K_2CO_3 (2.0 g, 14.1 mmol) and (isothiocyanatomethyl)benzene (
473 1.2 g, 8.0 mmol) in DMF: xylene (4:1) to get 1-(3-(Benzo[d]oxazol-2-yl)phenyl)-3-
474 benzylthiourea (1.9 g, 84%) as pale grey solid. M.p:210-212 ^{o}C. ^{1}H NMR (400 MHz, DMSO-
475 d_6): δ 9.27 (s, 1H), 9.01 (s, 1H), 8.44 (s, 1H), 7.92 (d, J = 8.0 Hz, 1H), 7.82 (t, J = 7.6 Hz, 2H),
476 7.68 (d, J = 8.0 Hz, 1H), 7.62 (t, J = 7.6 Hz, 1H), 7.58 (d, J = 8.4 Hz, 2H), 7.42–7.31 (m, 4H),
477 7.12 (t, J = 7.2 Hz, 1H), 5.04 (s, 2H); ^{13}C NMR (100 MHz, DMSO-d_6): δ 180.9, 166.8, 156.1,
478 144.3, 138.3, 136.2, 134.5, 134.0, 133.2(2C), 128.3, 127.4(2C), 125.3(2C), 125.1, 124.7, 123.6,
479 117.3, 112.5, 62.4. MS(ESI) *m/z* 360 $[M+H]^+$. Anal calcd for $C_{21}H_{17}N_3OS$: C, 70.17; H, 4.77;
480 N, 11.69%Found C, 70.28; H, 4.76; N, 11.71.

3.2.19. Synthesis of 1-(4-Fluorophenyl)-3-(3-(5-methylbenzo[d]oxazol-2-yl)phenyl)thiourea (17: The compound was synthesized according to above general procedure using 3-(5-methylbenzo[d]oxazol-2-yl)aniline (1.5 g, 6.69 mmol), K_2CO_3 (2.0 g, 14.1 mmol) and 1-fluoro-4-isothiocyanatobenzene (1.2 g, 7.8 mmol) in DMF: xylene (4:1) to get 1-(4-Fluorophenyl)-3-(3-(5-methylbenzo[d]oxazol-2-yl)phenyl)thiourea (2.1 g, 81%) as white solid. M.p:235-237 ^{o}C. ^{1}H NMR (400 MHz, DMSO-d_6): δ 10.27 (s, 2H), 8.49 (s, 1H), 7.84–7.74 (m, 3H), 7.62–7.44 (m, 5H), 7.09 (t, *J* = 7.6 Hz, 2H), 2.42 (s, 3H); ^{13}C NMR (100 MHz, DMSO-d_6): δ 182.4, 164.5, 160.2, 146.1, 142.3, 138.5, 135.6, 133.2, 131.4(2C), 130.9, 130.2, 128.2, 126.9, 125.6(2C), 124.3, 123.1, 118.4, 113.6, 22.5. MS(ESI) m/z 378 $[M+H]^+$. Anal calcd for $C_{21}H_{16}FN_3OS$: C, 66.83; H, 4.27; F, 5.03; N, 11.13 Found C, 66.90; H, 4.28; N, 11.15.

3.2.20. Synthesis of 1-(3-(benzo[d]oxazol-2-yl)phenyl)-3-(4-nitrophenyl)thiourea (18): The compound was synthesized according to above general procedure using 3-(5-methylbenzo[d]oxazol-2-yl)aniline (1.5 g, 6.69 mmol), K_2CO_3 (2.0 g, 14.1 mmol) and 1-isothiocyanato-4-nitrobenzene (1.2 g, 8.0 mmol) in DMF: xylene (4:1) to get 1-(3-(benzo[d]oxazol-2-yl)phenyl)-3-(4-nitrophenyl)thiourea (2.1 g, 85%) as yellow solid. M.p:236-238 ^{o}C. ^{1}H NMR (400 MHz, DMSO-d_6): δ 10.07 (s, 2H), 8.48 (s, 1H), 8.05 (d, *J* = 8.0 Hz, 2H), 7.92 (d, *J* = 7.6 Hz, 1H), 7.84 (t, *J* = 7.6 Hz, 2H), 7.65–7.58 (m, 3H), 7.48 (d, *J* = 8.0 Hz, 2H), 7.12 (t, *J* = 8.0 Hz, 1H); ^{13}C NMR (100 MHz, DMSO-d_6): δ 181.6, 163.4, 153.4, 143.8, 141.3, 139.3, 136.3, 134.5, 133.2, 132.9(2C), 130.4, 129.4, 128.6(2C), 127.2(2C), 125.3, 118.6, 116.1. MS(ESI) *m/z* 391 $[M+H]^+$. Anal calcd for $C_{20}H_{14}N_4O_3S$: C, 61.53; H, 3.61; N, 14.35 Found C, 61.58; H, 3.60; N, 14.37.

3.2.21. Synthesis of 1-(3-(benzo[d]oxazol-2-yl)phenyl)-3-(4-fluorophenyl)thiourea (19): The compound was synthesized according to above general procedure using 3-(benzo[d]oxazol-

2-yl)aniline (1.3 g, 6.19 mmol), K_2CO_3 (2.0 g, 14.1 mmol) and 1-fluoro-4-isothiocyanatobenzene (1.2 g, 7.6 mmol) in DMF: xylene (4:1) to get 1-(3-(benzo[d]oxazol-2-yl)phenyl)-3-(4-fluorophenyl)thiourea (1.9 g, 84%) as pale red solid. M.p:235-237 ^{o}C. ^{1}H NMR (400 MHz, DMSO-d_6): δ 9.67 (s, 1H), 9.21 (s, 1H), 8.46 (s, 1H), 7.94 (d, J = 8.0 Hz, 2H), 7.89 (d, J = 7.6 Hz, 1H), 7.72–7.58 (m, 4H), 7.24 (d, J = 8.0 Hz, 2H), 7.12 (d, J = 7.6 Hz, 2H); ^{13}C NMR (100 MHz, DMSO-d_6): δ 182.8, 164.2, 156.8, 144.4, 140.4, 138.2, 135.6, 133.9, 133.3, 132.3(2C), 130.2, 129.4, 128.2, 127.3(2C), 125.5, 124.2, 119.3, 115.2. MS(ESI) *m/z* 364 $[M+H]^+$. Anal calcd for $C_{20}H_{14}FN_3OS$: C, 66.10; H, 3.88; N, 11.56 Found C, 66.18; H, 3.87; N, 11.59.

3.2.22. Synthesis of 1-(3-(5-methylbenzo[d]oxazol-2-yl)phenyl)-3-(4-nitrophenyl)thiourea (20): The compound was synthesized according to above general procedure using 3-(5-methylbenzo[d]oxazol-2-yl)aniline (1.5 g, 6.69 mmol), K_2CO_3 (2.0 g, 14.1 mmol) and 1-isothiocyanato-4-nitrobenzene (1.1 g, 7.5 mmol) in DMF: xylene (4:1) to get 1-(3-(5-methylbenzo[d]oxazol-2-yl)phenyl)-3-(4-nitrophenyl)thiourea (2.2 g, 81%) as pale yellow solid. M.p:241-243 ^{o}C. ^{1}H NMR (400 MHz, DMSO-d_6): δ 9.47 (s, 1H), 9.03 (s, 1H), 8.41 (s, 1H), 8.09 (d, J = 8.0 Hz, 2H), 7.89 (d, J = 7.6 Hz, 1H), 7.87–7.74 (m, 3H), 7.69–7.56 (m, 2H), 7.36 (d, J = 8.0 Hz, 2H), 2.40 (s, 3H); ^{13}C NMR (100 MHz, DMSO-d_6): δ 182.9, 161.9, 150.3, 144.6, 142.0, 138.4, 136.0, 133.9, 133.2, 132.6(2C), 131.4, 128.9, 128.2(2C), 127.6, 126.5, 124.1, 117.9, 114.3, 21.9. MS(ESI) *m/z* 405 $[M+H]^+$. Anal calcd for $C_{21}H_{16}N_4O_3S$: C, 62.36; H, 3.99; N, 13.85 Found C, 62.48; H, 3.98; N, 13.87.

3.2.23. Synthesis of 1-(3-(5-methylbenzo[d]oxazol-2-yl)phenyl)-3-phenylthiourea (21): The compound was synthesized according to above general procedure using 3-(5-methylbenzo[d]oxazol-2-yl)aniline (1.5 g, 6.69 mmol), K_2CO_3 (2.0 g, 14.1 mmol) and

isothiocyanatobenzene (1.0 g, 7.4 mmol) in DMF: xylene (4:1) to get 1-(3-(5-methylbenzo[d]oxazol-2-yl)phenyl)-3-phenylthiourea (1.9 g, 79%) as grey solid. M.p:155-157 ^{o}C. ^{1}H NMR (400 MHz, DMSO-d_6): δ 10.26 (s, 2H), 8.41 (s, 1H), 7.94 (d, J = 8.0 Hz, 1H), 7.84–7.76 (m, 3H), 7.62 (d, J = 7.2 Hz, 2H), 7.46–7.35 (m, 3H), 7.22 (d, J = 7.6 Hz, 2H), 2.44 (s, 3H); ^{13}C NMR (100 MHz, DMSO-d_6): δ 183.5, 164.6, 148.3, 143.2, 137.4, 135.9, 135.0, 134.2, 133.8(2C), 130.4, 128.6, 128.2, 126.2(2C), 125.4, 124.3, 123.9, 118.2, 113.7, 22.3. MS(ESI) *m/z* 360 $[M+H]^+$. Anal calcd for $C_{21}H_{17}N_3OS$: C, 70.17; H, 4.77; N, 11.69% Found C, 70.28; H, 4.76; N, 11.67%.

3.2.24. Synthesis of 1-(4-chlorophenyl)-3-(3-(5-methylbenzo[d]oxazol-2-yl)phenyl)thiourea (22): The compound was synthesized according to above general procedure using 3-(5-methylbenzo[d]oxazol-2-yl)aniline (1.5 g, 6.69 mmol), K_2CO_3 (2.0 g, 14.1 mmol) and 1-chloro-4-isothiocyanatobenzene (1.3 g, 7.6 mmol) in DMF: xylene (4:1) to get 1-(4-chlorophenyl)-3-(3-(5-methylbenzo[d]oxazol-2-yl)phenyl)thiourea (2.1 g, 80%) as white solid. M.p:190-192 ^{o}C. ^{1}H NMR (400 MHz, DMSO-d_6): δ 10.45 (s, 2H), 8.48 (s, 1H), 7.96 (s, 1H), 7.89 (t, J = 8.0 Hz, 1H), 7.76 (d, J = 7.6 Hz, 1H), 7.56–7.48 (m, 4H), 7.26 (d, J = 7.6 Hz, 2H), 7.18 (t, J = 7.6 Hz, 1H), 2.41 (s, 3H); ^{13}C NMR (100 MHz, DMSO-d_6): δ 182.9, 163.9, 149.2, 143.6, 136.8, 135.4, 134.5, 133.2, 132.4(2C), 129.5, 127.8(2C), 127.2, 126.5, 125.3, 124.6, 124.2, 120.3, 116.4, 22.6. MS(ESI) *m/z* 394 $[M+H]^+$. Anal calcd for $C_{21}H_{16}ClN_3OS$: C, 64.03; H, 4.09; N, 10.67 Found C, 64.11; H, 4.10; N, 10.65.

3.2.25. Synthesis of 1-benzyl-3-(3-(5-methylbenzo[d]oxazol-2-yl)phenyl)thiourea (23): The compound was synthesized according to above general procedure using 3-(5-methylbenzo[d]oxazol-2-yl)aniline (1.5 g, 6.69 mmol), K_2CO_3 (2.0 g, 14.1 mmol) and (isothiocyanatomethyl)benzene (1.2 g, 7.9 mmol) in DMF: xylene (4:1) to get 1-benzyl-3-(3-

(5-methylbenzo[d]oxazol-2-yl)phenyl)thiourea (2.0 g, 79%) as grey solid. M.p:209-211 ^{o}C. ^{1}H NMR (400 MHz, DMSO-d_6): δ 9.46 (s, 1H), 9.21 (s, 1H), 8.34 (s, 1H), 8.21 (s, 1H), 7.83–7.74 (m, 3H), 7.63–7.48 (m, 2H), 7.31–7.24 (m, 5H), 5.01 (s, 2H), 2.43 (s, 3H); ^{13}C NMR (100 MHz, DMSO-d_6): δ 180.2, 163.7, 146.9, 142.3, 138.6, 134.7, 134.4, 133.8, 133.2(2C), 131.4, 127.6, 126.4, 125.9(2C), 125.3, 124.5, 123.6, 123.0, 119.6, 54.6, 23.1. MS(ESI) *m/z* 374 $[M+H]^+$. Anal calcd for $C_{22}H_{19}N_3OS$: C, 70.75; H, 5.13; N, 11.25 Found C, 70.88; H, 5.12; N, 11.27.

3.2.26. Synthesis of 1-(3-(5-methylbenzo[d]oxazol-2-yl)phenyl)-3-(p-tolyl)thiourea (24): The compound was synthesized according to above general procedure using 3-(5-methylbenzo[d]oxazol-2-yl)aniline (1.5 g, 6.69 mmol), K_2CO_3 (2.0 g, 14.1 mmol) and 1-isothiocyanato-4-methylbenzene (1.2 g, 7.9 mmol) in DMF: xylene (4:1) to get 1-(3-(5-methylbenzo[d]oxazol-2-yl)phenyl)-3-(p-tolyl)thiourea (2.1 g, 83%) as pale brown solid. M.p:231-233 ^{o}C. ^{1}H NMR (400 MHz, DMSO-d_6): δ 9.63 (s, 2H), 8.36 (s, 1H), 7.96 (d, J = 8.0 Hz, 1H), 7.89 (d, J = 7.6 Hz, 2H), 7.76 (d, J = 8.0 Hz, 1H), 7.64–7.56 (m, 3H), 7.26 (d, J = 8.0 Hz, 2H), 7.18 (d, J = 8.0 Hz, 1H), 2.44 (s, 3H), 2.41 (s, 3H); ^{13}C NMR (100 MHz, DMSO-d_6): δ 179.7, 162.4, 146.4, 144.4, 140.8, 138.6, 135.7, 135.3, 134.0, 133.9(2C), 131.4, 130.5, 129.3(2C), 127.5(2C), 124.8, 117.4, 115.2, 23.4, 22.5. MS(ESI) *m/z* 374 $[M+H]^+$. Anal calcd for $C_{22}H_{19}N_3OS$: C, 70.75; H, 5.13; N, 11.25 Found C, 70.83; H, 5.12; N, 11.23.

3.2.27. Synthesis of 1-(3-(benzo[d]oxazol-2-yl)phenyl)-3-(4-chlorophenyl)thiourea (25): The compound was synthesized according to above general procedure using 3-(benzo[d]oxazol-2-yl)aniline (1.3 g, 6.19 mmol), K_2CO_3 (2.0 g, 14.1 mmol) and 1-chloro-4-isothiocyanatobenzene (1.3 g, 7.7 mmol) in DMF: xylene (4:1) to get 1-(3-(benzo[d]oxazol-2-yl)phenyl)-3-(4-chlorophenyl)thiourea (1.9 g, 81%) as white solid. M.p:230-232 ^{o}C. ^{1}H NMR (400 MHz, DMSO-d_6): δ 10.23 (s, 2H), 8.39 (s, 1H), 7.90 (t, J = 8.0 Hz, 2H), 7.81 (d, J = 7.6

Hz, 2H), 7.56 (d, *J* = 8.0 Hz, 1H), 7.48 (d, *J* = 7.6 Hz, 1H), 7.36 (d, *J* = 8.0 Hz, 2H), 7.21–7.12 (m, 3H); ^{13}C NMR (100 MHz, DMSO-d_6): δ 182.7, 163.5, 144.7, 142.5, 139.8, 137.5, 134.8, 134.3, 134.1, 133.4(2C), 132.2, 131.4, 129.6(2C), 128.1, 126.4(2C), 118.6, 116.4. MS(ESI) *m/z* 380 $[M+H]^+$. Anal calcd for $C_{20}H_{14}ClN_3OS$: C, 63.24; H, 3.71; N, 11.06 Found C, 63.32; H, 3.70; N, 11.08.

3.2.28. Synthesis of 1-(3-(benzo[d]oxazol-2-yl)phenyl)-3-phenylthiourea (26): The compound was synthesized according to above general procedure using 3-(benzo[d]oxazol-2-yl)aniline (1.3 g, 6.19 mmol), K_2CO_3 (2.0 g, 14.1 mmol) and isothiocyanatobenzene (1.1 g, 8.1 mmol) in DMF: xylene (4:1) to get 1-(3-(benzo[d]oxazol-2-yl)phenyl)-3-phenylthiourea (1.7 g, 82%) as white solid. M.p:182-184 ^{o}C. ^{1}H NMR (400 MHz, DMSO-d_6): δ 10.01 (s, 2H), 8.43 (s, 1H), 7.93 (d, *J* = 8.0 Hz, 1H), 7.81 (t, *J* = 7.6 Hz, 2H), 7.20 (d, *J* = 7.6 Hz, 1H), 7.54 (t, *J* = 8.0 Hz, 1H), 7.49 (d, *J* = 8.0 Hz, 2H), 7.45–7.30 (m, 4H), 7.15 (t, *J* = 8.0 Hz, 1H); ^{13}C NMR (100 MHz, DMSO-d_6): δ 179.8, 164.6, 152.3, 146.4, 143.4, 140.3, 131.2, 129.2 (2C), 128.3, 127.1, 126.3, 125.1, 124.6, 124.2 (2C), 123.8, 123.2, 120.4, 112.7. MS(ESI) *m/z* 346 $[M+H]^+$. Anal calcd for $C_{20}H_{15}N_3OS$: C, 69.54; H, 4.38; N, 12.17 Found C, 69.63; H, 4.37; N, 12.19.

3.2.29. Synthesis of 1-(3-(benzo[d]oxazol-2-yl)phenyl)-3-(p-tolyl)thiourea (27): The compound was synthesized according to above general procedure using 3-(benzo[d]oxazol-2-yl)aniline (1.3 g, 6.19 mmol), K_2CO_3 (2.0 g, 14.1 mmol) and 1-isothiocyanato-4-methylbenzene (1.2 g, 7.9 mmol) in DMF: xylene (4:1) to get 1-(3-(benzo[d]oxazol-2-yl)phenyl)-3-(p-tolyl)thiourea (1.9 g, 81%) as pale brown solid. M.p:221-223 ^{o}C. ^{1}H NMR (400 MHz, DMSO-d_6): δ 10.21 (s, 2H), 8.37 (s, 1H), 7.87 (d, *J* = 8.0 Hz, 1H), 7.78–7.64 (m, 3H), 7.60–7.47 (m, 5H), 7.27 (t, *J* = 7.6 Hz, 2H), 2.43 (s, 3H); ^{13}C NMR (100 MHz, DMSO-d_6): δ 176.4, 163.3, 152.1, 144.7, 138.3, 138.0, 136.7, 136.1, 135.3, 133.3(2C), 132.6, 132.0,

129.3(2C), 127.2, 126.6, 125.3, 120.4, 116.8, 22.3. MS(ESI) *m/z* 360 $[M+H]^+$. Anal calcd for $C_{21}H_{17}N_3OS$: C, 70.17; H, 4.77; N, 11.69 Found C, 70.26; H, 4.76; N, 11.71.

4.3. In vitro glutamate racemase activity assay

4.3.1. Expression and purification of GR from M. tuberculosis and B. subtilis:

The recombinant genes coding for *Mtb* H37Rv and *Bsb subsp. subtilis* 168 glutamate racemase were PCR amplified using an expression plasmid pET28a+ with N-terminal histidine tags and an expression vector E.*coli* BL21 (DE3) cells. Ni±NTA metal-affinity column (His-bind resin, Novagen) was used for purification of GR by using wash buffer (20 mM TEA, 10 mM $MgCl_2$, 10 % glycerol, 500 mM NaCl, 50 mM imidazole, 1 mM DTT, 1 mg/mL lysozyme, 0.1 mM phenyl methane sulfonyl fluoride, pH 7.8). The pure enzyme was obtained after running the column with 500 mM imidazole in wash buffer. Purity of protein was confirmed using SDS-PAGE. The protein was stored in aliquots at -80^{o}C and single time thawed protein was used for analysis [8, 9].

4.3.2. Inhibitory activity screening of compounds:

Inhibitory activity testing of synthesized compounds was carried out using a coupled assay, a 100 µL mixture consisting of 100 mM Tris–HCl pH 8.0, 5 mM NAD+, 1 mM D-Glutamate, 10 U/mL L-glutamate dehydrogenase (LDH) (all the chemicals were procured from Sigma) and enzyme concentration of 1µM *Bsb* glutamate racemase at different concentrations (50µM to 0.5µM) of compounds monitored at 340 nm using microplate spectrophotometer (Spectromax M4, Molecular devices). IC_{50} was determined by measuring the NADH conversion from NAD+ at 340nm [8].

4.4. Molecular docking simulations:

Molecular docking and simulations studies on D-glutamate bound glutamate racemase of *Mtb* (PDB ID: 5HJ7) and *Bsb* (PDB ID: 1ZUW) were performed using Schrodinger software. Crystal structures were retrieved from protein data bank. Sitemap was utilized to generate allosteric sites and ranked according to their scores, volume and sizes. The protein was prepared with the help of Protein Preparation Wizard of Schrödinger Suite 9.3 [10]. Protein was optimized and minimized using OPLS_2005 (optimized potential for liquid simulations) force field and grids were generated using Glidegrid. The D-glutamate and test compounds were energy minimized using Ligprep module. The generated grid files from the prepared proteins and minimized test compounds were used for Glide XP docking calculations. XP descriptor and RMSD calculator were enabled. The XP Glide scoring function was used to get the best ranked compounds and the specific interactions like H-bonds, *π-cation* and *π-π* stacking were analyzed using XP visualizer in Glide module. Molecular dynamics (MD) simulations for 10 ns and calculations of active ligand bound to crystal structures were run in Desmond using OPLS_2005 force field to study the stability pattern in solvent system environment. Defining simulation parameters, calculation of RMSD, RMSF profiles were carried as reported in literature [11, 12].

4.5. In vitro M. tuberculosis assay (active model):

Synthesized compounds were screened for activity against replicating *Mtb* H37Rv bacteria by determining their minimum inhibitory concentration (MIC) using microplate Alamar blue assay method (MABA) [13]. *Mtb* culture in middlebrook 7H9 broth with 10% OADC (0.1% casitone, 0.5% glycerol, supplemented oleic acid, albumin, dextrose, and catalase) (Himedia) having OD_{590} 1.0 was diluted in1:20 of which 100 µL culture was used as inoculums for screening. Each thawed test compound stock solutions was diluted in middlebrook 7H9 broth by four-fold the final highest concentration to be tested. Compounds were diluted serially in a sterile 96-well

641 microtiter plates using 100 µL middlebrook 7H9 broth. Positive and negative controls were also
642 plated. All the sampling was done in duplicates. Further readings were compared against the
643 standards namely Rifampicin, Ethambutol and Isoniazid. Humidity was maintained during
644 incubation period by adding sterile water into all the boundary wells of each plate. The plates
645 were incubated at 37 ^{o}C for a week. After incubation period, 30 µL of Alamar blue solution was
646 added to each well, and the plate was re-incubated for 12 h. Growth is indicated by the a color
647 change from blue to pink and the lowest concentration of compound that prevented the color
648 change was noted as its MIC. Inhibitor susceptibility testing in the presence of verapamil and
649 piperine was done with concentrations 50 µg/mL and 8 µg/mL respectively same as above
650 described procedure [27].

651 ***4.6. Nutrient starvation model:***

652 *Mtb* (H37Rv) culture starved in PBS (phosphate buffered saline) for 6 weeks was used for the
653 assay. Dormant stage attained bacteria was tested with test and standard compounds for their
654 activity for 7 days at a concentration of 10 µg/mL. After a week cell suspensions were diluted10-
655 fold using Middlebrook 7H9 broth with 10% OADC, further 100 µL of each dilution was plated
656 in sterile 48 well plates containing 450 µL of Middlebrook 7H9 broth in triplicates. The plates
657 were kept for incubation at 37^{o}C for four weeks. Wells with visible bacterial growth were
658 counted as positive, and most probable number (MPN) values were calculated using standard
659 statistical methods [14].

660 ***4.7. Kill Kinetics:***

661 *Mtb* culture with OD_{590} 0.6-1.0 was centrifuged at 2500 rpm (Sorvall ST 16R centrifuge) for
662 about 15 minutes. The cell pellet was diluted with 10% PBS-Tyloxapol until the OD_{590} reaches
663 0.1, followed by depleting nutrients for two weeks. Tubes were labeled with the control

(DMSO), inhibitor with test concentrations (5, 10 and 20 µM). To each tube, 5 mL of PBS-Tyloxapol and 50 µL of starved culture were added. To test drug tubes 100 µL of stock solution (50x) of compound was added to attain desired final concentration. To control tube was added with 100 µL DMSO. The contents in tubes were mixed and incubated at 37 ^{o}C. The treated cell suspensions were plated for inhibitory activity at 0, 7, 14, 21 day intervals for each concentration of test compounds. The bacterial count was calculated using standard statistical methods employing MPN assay [15].

4.8. Biofilm:

4.5 mL of Sautons media (HiMedia) was added in each well into a sterile 12 well plate with the *Mtb* culture with A_{590} between 0.7-1.0. Biofilm was developed within five weeks of incubation at 37 ^{o}C. To the matured biofilm test compound was added at desired concentration and swirled (n = 4) and sealed. After a week of incubation, tween-80 (0.1% v/v) was added, swirled at room temperature for about 15 minutes. The contents of each well were centrifuged and pellet was suspended in 5 mL of wash buffer (PBS with 10% glycerol and 0.05% Tween-80) and washed for three times. Finally, the pellet was re-suspended in 5 mL of wash buffer and kept on rocking overnight at room temperature. Contents were homogenized through syringe passage for 5 times. The persistence of bacteria in the biofilm population was determined by comparing antibiotic treated plates with positive control plates by MPN assay [16].

4.9. In vivo activity assay in zebrafish:

In vivo assay was carried out in zebrafish infected with *Mycobacterium marinum* (ATCC BAA-535) a genetic relative of *Mtb.* Most active compound from *in vitro* assays was tested by incubating bacteria at 30 ^{o}C in Middlebrook 7H9 broth. Fishes were sorted into control and treatment groups (n = 6) according to their weights. All the groups were infected by

intraperitoneal route with 20 µL of bacterial culture (around 0.75 million bacterial cells) for a week maintaining chamber temperature at 25^{o}C. Once the infection has developed, fishes were administered with test drug (10 mg/kg dose) orally for a 7 day treatment period, same with standard (for INH 5 mg/kg). After treatment period the fishes were suspended in Kanamycin treated water for 10 minutes to kill exogenous bacteria on fish skin. Further fishes were sacrificed and the tissue was homogenized and sample was prepared in Middlebrook 7H9 broth and plated for bacterial growth. The plates were checked for bacterial count using MPN assay method [17].

4.10. Cytotoxicity determination:

The cell toxicity study of synthesized compounds was tested with inhibition assay on mouse macrophage cell line (RAW 264.7) [18]. In sterile 96 well microtiter plate $5x10^3$ cells in each well were plated and incubated at different concentrations of compounds for 48 h at 37^{o}C [19]. After the incubation period 10 µL of 3-(4,5-Dimethylthiazol-2-yl)-2,5-Diphenyltetrazolium Bromide (MTT reagent) (10 mg/mL) was added and incubated for 3h more. After 3h, media was removed and 200 µL of DMSO was added to each well. DMSO dissolves the formazan crystals formed in wells. The absorbance was measured at 560nm using Perkin Elmer Victor X3 microplate reader against the blank. The assay was performed in triplicates for each concentration. The cytotoxicity was represented as % inhibition at each particular concentration.

Acknowledgements

P.M. is thankful to Department of Science and Technology, Government of India for the Inspire fellowship. DS is thankful to Department of Biotechnology, Government of India for the Tata innovation fellowship (BT/HRD/35/01/04/2015).

References

1. K.B. Urdahl, S. Shafiani, J.D. Ernst. Mucosal Immunol. 4 (2011) 288–293.

711 2. A.J. Wolf, L. Desvignes, B. Linas, N. Banaiee, T. Tamura, K. Takatsu, J.D. Ernst. J Exp Med
712 205 (2008) 105–115.

713 3. V. Balasubramanian, M.S. Pavelka, S.S. Bardarov, J. Martin, T.R Weisbrod, R.A. McAdam,
714 BR Bloom, WR Jacobs, Jr Allelic. J Bacteriol. 178 (1996) 273–279.

715 4. A. Israyilova , S. Buroni, F. Forneris, V.C. Scoffone, N.Q. Shixaliyev, G. Riccardi.
716 PLoS ONE. 11 (2016): e0167350.

717 5. B. Geng, G. Basarab, J. Comita-Prevoir, M. Gowravaram, P. Hill, A. Kiely. Bioorg Med
718 Chem Lett. 19 (2009) 930-936.

719 6. A. Ciulli, Methods Mol Biol. 1008 (2013) 357–388.

720 7. A.F. Rudolf, T. Skovgaard, S. Knapp, L.J. Jensen, J. Berthelsen. PLoS ONE. 9 (2014)
721 e98800.

722 8. S. Poen, Y. Nakatani, H.K. Opel-Reading, M. Lassé, R.CJ. Dobson, K.L. Kraus. Biochem J.
723 473 (2016) 1267–1280.

724 9. G.A. Prosser, A. Rodenburg, H. Khoury, C. de Chiara, S. Howell, A.P. Snijders, L.P. de
725 Carvalho. Antimicrob Agents Chemother. 60 (2016) 6091-6099.

726 10. Schrödinger Suite 2012 Protein Preparation Wizard; Epik, *v*2.2, Schrödinger, LLC, New
727 York, NY, 2012; Impact, *v*5.7, Schrödinger, LLC, New York, NY, 2012; Prime *v*2.3,
728 Schrödinger, LLC, New York, NY, 2012.

729 11. V. Kräutler, W.F. van Gunsteren, P.H. Hünenberger. J. Comput. Chem. 22 (2001) 501-508.

730 12. P. Suryadevara, P. Yogeeswari, V. Soni, P.B. Devi, V.K. Nandicoori, D. Sriram. Curr Top
731 Med Chem. 16 (2016) 978-995.

732 13. F. Reck, R. Alm, P. Brassil, J. Newman, B. Dejonge, C.J. Eyermann, G. Breault, J. Breen, J.
733 Comita-Prevoir, M. Cronin, H. Davis, D. Ehmann, V. Galullo, B. Geng, T. Grebe, M.
734 Morningstar, P. Walker, B. Hayter, S. Fisher, J. Med. Chem. 54 (2011) 7834e7847.14.

735 14. J.C. Betts, P.T. Lukey, L.C. Robb, R.A. McAdam, K. Duncan. Mol Microbiol. 43 (2002)
736 717–731.

737 15. T. Parish, N.G. Stoker. Mycobacteria Protoc. (1998) 269–279.

738 16. K. Kulka, G. Hatfull, A.K. Ojha. J Vis Exp. 60 (2012) 3820.

739 17. R.C. Mark, M.T. David. Disease Models & Mechanisms. 7 (2014) 777-784.

740 18. F. Reck, R.A. Alm, P. Brassil, J.V. Newman, P. Ciaccio, J. McNulty, H. Barthlow, K. Goteti,
741 J. Breen, J. Comita-Prevoir, M. Cronin, D.E. Ehmann, B. Geng, A.A. Godfrey, S.L .Fisher. J.
742 Med. Chem. 5 (2012) 6916–6933.

743 19. P. S. Charifson, A. L. Grillot, T. H.Grossman, J. D. Parsons, M. Badia, S. Bellon, D. D.
744 Deininger, J. E. Drumm, C. H. Gross, A. LeTiran, Y. Liao, N. Mani, D. P. Nicolau, E. Perola, S.
745 Ronkin, D. Shannon, L. L.Swenson, Q. Tang, P.R. Tessier, S.K. Tian, M. Trudeau, T. Wang, Y
746 Wei, H. Zhang, D. Stamos. J. Med. Chem. 51 (2008) 524327-524332.

747 20. C.H. Luan, S.H. Light, S.F. Dunne, W.F. Anderson. Methods Mol Biol. 1140 (2014) 263-
748 289.

749 21. M. Karplus, J.A. McCammon. Nat Struct Biol. 9 (2002) 646-652.

750 22. J. Venkatraman, J. Bhat , S.M. Solapure, J. Sandesh, D. Sarkar, S. Aishwarya, K. Mukherjee,
751 S. Datta, K. Malolanarasimhan,B. Bandodkar, K.S. Das. J Biomol Screen. 17 (2012) 293-302.

752 23. S. Cho, H.S. Lee, S. Franzblau. Methods Mol Biol. 1285 (2015) 281-292.

753 24. S. Molloy. Nat Rev Microbiol. 6 (2008) 500.

754 25. L.M. van Leeuwen, A.M. van der Sar, W. Bitter. Cold Spring Harb Perspect Med. 20 (2014)
755 a018580.

756 26. E.D. Rossi, J. A. Ainsa, G. Riccardi. FEMS Microbiol. Rev. 30 (2006) 36– 52.

757 27. S. Alibert S, J.M. Pages. *Expert Opin. Ther. Pat.* 17 (2007) 883-888.

758 28. J. D. Szumowski, K.N. Adams, P.H. Edelstein, L. Ramakrishnan. *Current topics in*
759 *microbiology and immunology*. (2013) 374-399.

760 29. S. Sharma, M. Kumar, S. Sharma, A. Nargotra, S. Koul, I.A. Khan. *J Antimicrob Chemother*.
761 65 (2010) 1694-170.

762 30. M. S.Vasava, M. N. Bhoi, S. K. Rathwa, M. A. Borad, S. G. Nair, H. D. Pate . *Indian J*
763 *Tuberc.* 64 (2017) 252-275.

764 31. M. W.Marney, R. P.Metzger, D. Hecht, F.Valafa. *Tuberculosis*. (In Press)

CAPTION FOR FIGURES AND TABLES

Fig. 1: (A) (Left): Melt curves of *Mtb* in its free state, bound with substrate and ligand. (Right) represents the melt temperature plotting derivative fluorescent (Y-axis) and temperature (X-axis). T_m can be measured from the minimum of the plot. (B) 3D representation of *Bsb* glutamate racemase crystal structure, employed for *in vitro* activity assay. (C) Structure of identified **lead 1** with melt temperature and IC_{50} value.

Scheme 1: Synthetic scheme utilized for synthesis of target molecules. Reagents and conditions: (a) PPA, 185 °C, 6h; (b) R^2-NCO, DIPEA, DMF, rt, 2h; (c) R^2-NCS, DMF/xylene(4:1), K_2CO_3, MW, 110 °C, 30minutes.

Table 1: Synthesized compounds represented with substitutions along with their biological activities

Fig. 2. Log dose response curve of compound **22.**

Fig. 3. Docking pose of active molecule **22** in **site 1** of *Mtb* (5HJ7) and *Bsb* (1ZUW) in superimposed view. Grey color represents protein and ligand in 5HJ7 whereas green represents 1ZUW.

Fig. 4. Binding pose and the interaction pattern of the compound **22** in A) *Mtb* and B) *Bsb*.

Fig. 5. Thermal stability curves of *Mtb* GR depicting the non-competitive inhibition by compound **22.** (A) Represents the melt curve of protein with D-glu and compound **22** (B) indicates the melt peaks where melt temperature can be determined.

784 **Fig. 6.** Activity profile of compounds in nutrient starved stress model. Bacterial count was
785 estimated through MPN (most probable number) assay and significance plot was developed by
786 adopting two way ANOVA ($p < 0.0001$, using GraphPad Prism Software).

787 **Fig. 7.** Kill kinetic curve of compound **22** depicting time dependant kill kinetics.

788 **Fig. 8.** Comparative biofilm inhibitory activity plots of compounds **17, 18, 19**, **25** and standard
789 drugs against *Mtb*. Bacterial count estimation (Mean ± S.D., n = 4) for control and treated
790 groups was conducted by using the MPN assay.

791 **Fig. 9.** Bacterial count estimation (Mean ± S.E.M., n = 6) for control and treated groups by zebra
792 fish model conducted by using MPN assay. Statistical significance has been analyzed by Two-
793 way ANOVA using GraphPad Prism Software.

Highlights:

- Lead for MTB Glutamate racemase identified using thermal shift assay
- Twenty-seven compounds synthesized based on lead 1.
- Compound **22** showed an IC_{50} of 1.1±0.52 µM
- It also exhibited good activity in MTB models